Electrocorticography reveals beta desynchronization in the basal ganglia-cortical loop during rest tremor in Parkinson's disease

Salman E. Qasim, BA[1], **Coralie de Hemptinne, PhD**[2], **Nicole C. Swann, PhD**[2], **Svjetlana Miocinovic, MD, PhD**[3], **Jill L. Ostrem, MD**[3], and **Philip A. Starr, MD, PhD**[2]

Coralie de Hemptinne: Coralie.Dehemptinne@ucsf.edu; Nicole C. Swann: Nicole.Swann@ucsf.edu; Svjetlana Miocinovic: Svjetlana.Miocinovic@ucsf.edu; Jill L. Ostrem: Jill.Ostrem@ucsf.edu; Philip A. Starr: Philip.Starr@ucsf.edu

[1]Department of Biomedical Engineering, Columbia University

[2]Department of Neurological Surgery, University of California San Francisco, San Francisco, CA, USA

[3]Department of Neurology, University of California San Francisco, San Francisco, CA, USA

Abstract

The pathophysiology of rest tremor in Parkinson's disease (PD) is not well understood, and its severity does not correlate with the severity of other cardinal signs of PD. We hypothesized that tremor-related oscillatory activity in the basal-ganglia-thalamocortical loop might serve as a compensatory mechanism for the excessive beta band synchronization associated with the parkinsonian state. We recorded electrocorticography (ECoG) from the sensorimotor cortex and local field potentials (LFP) from the subthalamic nucleus (STN) in patients undergoing lead implantation for deep brain stimulation (DBS). We analyzed differences in measures of network synchronization during epochs of spontaneous rest tremor, versus epochs without rest tremor, occurring in the same subjects. The presence of tremor was associated with reduced beta power in the cortex and STN. Cortico-cortical coherence and phase-amplitude coupling (PAC) decreased during rest tremor, as did basal ganglia-cortical coherence in the same frequency band. Cortical broadband gamma power was not increased by tremor onset, in contrast to the movement-related gamma increase typically observed at the onset of voluntary movement. These findings suggest that the cortical representation of rest tremor is distinct from that of voluntary movement, and support a model in which tremor acts to decrease beta band synchronization within the basal ganglia-cortical loop.

Corresponding author. Salman Qasim, Columbia University, 116th St & Broadway, New York, NY 10027, salman.qasim@columbia.edu.

INTRODUCTION

Parkinson's disease (PD) is a movement disorder characterized by severe loss of
dopaminergic neurons in the midbrain. This manifests in several cardinal symptoms
including a 4–7 Hz tremor at rest, rigidity, bradykinesia, and postural instability (Hoehn and
Yahr, 1967). Though many early studies searched for a single "generator" of tremor activity,
it is now thought that rest tremor emerges from changes in the network dynamics of the
basal ganglia-thalamocortical loop and cerebello-thalamocortical loop (Helmich et al.,
2012). Tremor related oscillatory activity has been observed throughout these networks,
through single unit recording (Hutchison et al., 1997; Levy et al., 2002; Levy et al., 2000
2002b) and local field potentials in the subthalamic nucleus (Reck et al., 2009; Weinberger
et al., 2009), and in mapping of cortical connectivity through the use of
magnetoencephalography (MEG) (Hirschmann et al., 2013; Timmermann et al., 2003;
Volkmann et al., 1996) and electroencephalography (EEG) (Hellwig et al., 2000). However,
most previous studies have recorded only from basal ganglia or cortex rather than studying
the simultaneous activity necessary to observe network changes corresponding to rest
tremor.

An understanding of the pathogenesis of rest tremor may provide insight into several
mysteries related to the clinical presentation of tremor in patients with PD. Unlike other PD
symptoms, such as bradykinesia or rigidity, the severity of tremor does not correlate with
dopaminergic cell death in the striatum (Pirker, 2003). It also does not correlate with the
severity of the other motor symptoms (Deuschl et al. 2000, 2001). Tremor-dominant patients
have slower progression of disability and better prognosis than patients without tremor
(Hoehn and Yahr, 1967). These characteristics suggest a pathophysiological distinction
between PD with rest tremor and PD without rest tremor. Recent authors have postulated
that these distinctions may indicate a compensatory role for rest tremor (Zaidel et al., 2009;
Helmich et al., 2012). One theory of parkinsonian bradykinesia implicates excessive
neuronal synchronization in the beta (13–30 Hz) band within and between structures of the
motor network (Hammond et al., 2007), and detailed examination of the network changes
underlying rest tremor would clarify whether rest tremor is acting to counter this
pathological synchronization.

In this study we examined the hypothesis that transient spontaneous epochs of rest tremor
may reflect a state of desynchronization in frequency bands other than tremor frequency,
within and between nuclei of the basal ganglia-thalamocortical motor loop. We approached
this using the technique of electrocorticography (ECoG) of sensorimotor cortex, combined
with subthalamic nucleus (STN) local field potential (LFP) recording, during spontaneous
epochs of rest tremor and rest without tremor, in PD patients undergoing surgical
implantation of deep brain stimulator (DBS) leads in the awake state. We found that tremor

is associated with a reduction in cortical and subthalamic beta power, cortico-cortical coherence, cortical-subthalamic coherence and cortical cross frequency coupling. These findings suggest that tremor acts to counter the excessive beta synchronization associated with parkinsonian bradykinesia. Our findings also have implications for the development of closed-loop stimulation algorithms that rely on biomarkers modulated by tremor.

MATERIALS AND METHODS

Subject Recruitment

The subjects in this study were recruited from a population of patients undergoing DBS implantation at one of two campuses: the University of California, San Francisco (UCSF), or the San Francisco Veteran Affairs Medical Center (SFVAMC). Each subject had a diagnosis of idiopathic Parkinson's disease confirmed by a movement disorders neurologist. Informed consent for the temporary intra-operative placement of the cortical strip was obtained prior to surgery under a protocol approved by the Institutional Review Board, according to the Declaration of Helsinki. Data from some of the same subjects in this study were also used, for different analyses, in other publications (Crowell et al., 2012; de Hemptinne et al., 2013, 2015; Shimamoto et al., 2013).

Surgery and placement of subdural ECoG electrodes and STN DBS lead

ECoG was recorded using either a 6-contact (n = 22) or 28-contact (n = 5) ECoG strip temporarily placed over the sensorimotor cortex (Panov et al., 2015). The ECoG strip was inserted under the dura through the burr hole used for the DBS lead placement and advanced in the direction of the intended target location, the arm area of motor cortex (3 cm from the midline, on the medial aspect of the "hand knob") (Yousry et al., 1997). Six-contact electrodes were composed of platinum contacts of 4 mm total diameter, 2.3 mm exposed diameter and 10 mm spacing between contacts (Integra NeuroScience, Plainsboro, NJ, or Ad-Tech, Racine WI)). Twenty-eight-contact electrodes were composed of platinum contacts of 2 mm total diameter, 1.2 mm exposed diameter and 4 mm spacing between contacts (Ad-Tech, Racine, WI).

Localization of the M1 contact was determined both anatomically and functionally. Anatomical localization was determined using either intraoperative computed tomography (iCT) merged with pre-operative MRI or lateral fluoroscopy as previously described (Crowell et al., 2012). Functional localization was performed with somatosensory potentials evoked by median nerve stimulation and used to select contacts for the subsequent analyses (frequency = 2Hz, pulse width = 200 μsec, pulse train length = 160 μsec, amplitude 25–40 mA). The central sulcus was localized using the N20 reversal technique (Crowell et al., 2012). The most posterior contact pair showing a reversed N20 potential was defined as the closest electrode pair to M1, the contact pair immediately posterior to that was defined as covering the central sulcus, and the contact pair posterior to that with an upward N20 waveform was defined as the closest electrode pair to primary somatosensory cortex (S1). These methods are illustrated in Figure 1.

DBS electrodes were placed in the STN as previously described (Starr et al., 2002). Targeting was confirmed by evaluation of stimulation induced symptom improvement and adverse effects, as well as by visualization of DBS lead location on an iCT scan computationally fused to the preoperative MRI (Shahlaie et al., 2011).

Intraoperative Data Collection

ECoG potentials were recorded using the Guideline 4000 system (FHC Inc, Bowdoin, ME) (n =7), the Alpha Omega Microguide Pro (Alpha Omega, Inc, Nazareth, Israel) (n = 14), or the PZ5 Neurodigitizer (Tucker Davis Technologies, Inc., Alachua, FL) (n= 6). ECoG potentials recorded with the 6-contact strips were recorded in a bipolar configuration referencing the five most posterior contacts (contacts 1–5) to the most anterior one. With the 28-contact strip, ECoG potentials were referenced to a scalp needle electrode.

Subcortical local field potentials were recorded using a 4-contact cylindrical DBS lead (Model 3389, Medtronic, Inc, Minneapolis MN). Each contact was 1.5 mm in height and 1.2 mm in diameter, with 0.5 mm intercontact spacing. With contact 0 as the most ventral contact and contact 3 as the most dorsal contact, LFPs were recorded using contacts 1 and 2. Subcortical LFPs from subjects implanted with the 6-contact ECoG strips were recorded in a bipolar configuration while subcortical LFPs from subjects implanted with the 28-contact strips were recorded in a monopolar configuration and re-referenced in a bipolar configuration in post-processing.

Six-contact ECoG and subcortical LFP signals were bandpass filtered 1–500 Hz, amplified $\times$ 7000. All signals were recorded at a sampling rate of minimum 1 KHz and up to 3 KHz. All data recordings after lead insertion were performed 5 to 60 minutes after insertion in order to minimize the contribution of acute effects related to electrode placement (Mann et al., 2009; Tykocki et al., 2013). The Guideline system had slight attenuation up to 20 Hz due to the slow roll-off characteristics of an intrinsic 1 Hz high pass filter, and this was compensated for using an empirically determined correction factor (Crowell et al., 2012). Even so this did not consistently correct for attenuation below 4 Hz. When results were analyzed separately for data collected with the GS4000, no differences were found in any condition. Nevertheless, we discarded frequencies below 4 Hz for group comparisons.

Additional channels were used to record analog signals from surface electromyography (EMG) from the arm contralateral to the cortical strip over the extensor carpi radialis (ECR) and/or biceps brachii. We also recorded the same hand's movement in three-dimensional space with a tri-axial accelerometer affixed to the wrist (AX2300-365, FHC, Inc, Bowdoin, ME). These data were recorded at a sampling rate of minimum 1 KHz and up to 25 KHz.

Subjects were lying in a semi-supine position in the operating room for the duration of surgery and data collection, and instructed to keep their eyes open and refrain from speech or voluntary movements during recordings. Data were recorded in two conditions: during rest tremor and rest without tremor.

Pre-Processing

All data were processed and analyzed offline in MATLAB (Mathworks, Inc). All the data were downsampled to 1 KHz and notch filtered for power line noise (60 Hz) and its harmonics (at 120, 180, 240 Hz).

DATA ANALYSIS

Identification of Tremor Epochs

In order to identify epochs of tremor, we collected surface EMG and accelerometry data from subjects' contralateral arm. Due to a high signal to noise ratio in the EMG data, residual activation of extraneous muscle groups, and possible bias from sampling only a proportion of arm muscle, the accelerometer data were used for the clearest possible discrimination of tremor epochs (Cagnan et al., 2014) while EMG was used to confirm the presence of muscle activity during those epochs. We identified the epochs of tremor and rest through visual identification of 4–7 Hz rhythmic changes in accelerometer amplitude. Precise tremor onset and offset was not always clearly identifiable due to the gradual, low amplitude manner in which tremor may often arise. Due to this difficulty in identifying a precise onset, we selected data segments for which accelerometry showed at least 6 seconds of clearly identifiable tremor bounded by at least 1 second of identifiable tremor before and after to ensure there was no ambiguity about the presence of tremor. These epochs were used for all analyses, with the exception of cross-frequency coupling analyses. These analyses required longer epochs of rest and tremor available in a subset of patients (described below).

Spectral Power

Power spectral density was calculated using Welch's method (MATLAB function pwelch) with a 50% overlap, resulting in a frequency resolution of approximately 1 Hz and was log transformed for all comparisons. Peaks in the resulting spectrogram were recorded and log power was also averaged across frequency bands: theta (4–8 Hz), alpha (8–13 Hz), low beta (12–20 Hz), beta (13–30 Hz), high beta (20–30 Hz), low gamma (30–55 Hz), gamma (30–80 Hz), and broadband gamma (80–200 Hz).

The amplitude of the beta peak was analyzed by fitting a 5th order polynomial to the PSD with the beta peak removed to establish a baseline, while the width of the beta peak was evaluated by modeling the beta peak as a Gaussian curve and calculating the standard deviation.

Coherence

Coherence (magnitude-squared coherence) was calculated using Welch's averaged modified periodogram method with a 1 s window and a frequency resolution of 1 Hz (MATLAB function mscohere). Coherence was analyzed along a spectrum of frequencies, and averaged across the aforementioned frequency bands as well as any additional sub-divisions of interest. Comparisons were made between peaks in the coherence spectrum as well as between averaged coherence in a given frequency band. Peak coherence was evaluated using local maximums in the coherence spectrum that exceeded the threshold determined by surrogate analysis (see "Statistical Analysis").

Phase Synchrony Index (PSI) and Amplitude-Amplitude Coupling (AAC)

Phase synchrony, unlike magnitude squared coherence, is a measure of consistent phase difference or amount of "phase locking" that occurs between two signals, without taking into account any amplitude relationships (Mormann et al., 2000). Amplitude-amplitude coupling (AAC) is a measure of the correlation between amplitude envelopes independent of phase interactions (Bruns et al., 2000). These two connectivity measures were calculated using custom MATLAB functions. First, each signal was bandpass filtered around the frequency band of interest using a two way, least squares FIR filter (eegfilt from EEGLAB toolbox) ((Delorme and Makeig, 2004). Phase information was extracted from each filtered signal using the Hilbert transform, and was used to calculate the phase difference, φ. The angular phase difference distribution was obtained by transforming φ onto the unit circle in the complex plane using Euler's formula. The mean of this distribution is the phase synchrony index (PSI), where:

$$PSI = \left| \frac{1}{N} \sum_{j=0}^{N-1} e^{\varphi_{n,m}(j\Delta t)} \right|.$$

The amplitude envelope for each signal was calculated by taking the square root of the squared signal plus the squared Hilbert transform of the signal:

$$A(x) = \sqrt{x(t)^2 + |H(x(t))|^2}$$

Here, x(t) is the bandpass filtered signal, and H(x(t)) is the Hilbert transform of the filtered signal. Then, Pearson's correlation coefficient was calculated between the amplitude envelopes over the course of each epoch. This correlation coefficient was squared in order to make it more comparable to magnitude-squared coherence.

Cortical cross frequency AAC was calculated in a subset of subjects (n = 9) who experienced a long enough epoch of tremor to reliably assess the relationship between low and high frequency activity (~30 seconds, uninterrupted). Uninterrupted epochs were selected in order to minimize artifactual coupling stemming from edge effects. STN and STN-M1 AAC were calculated in a different subset of patients (n = 8) who experienced long epochs of rest and tremor after lead insertion.

Phase-Amplitude Coupling (PAC)

Phase-amplitude coupling (PAC) quantifies the relationship between the phase of one frequency band and the amplitude of another, either within an area or between areas. This methodology is described by Tort et al., (2010) and application to our data is detailed in our prior work (de Hemptinne et al., 2013, 2015). Briefly, the signal was bandpass filtered for both low frequency (4–40 Hz, with a bin bandwidth of 2 Hz) and high frequency (40–400, with a bin bandwidth of 4 Hz) components. The phase of the low frequency components and the amplitude of the high frequency components were extracted using the Hilbert transform. The distribution of the instantaneous amplitude envelope was computed for every 20° interval of the instantaneous phase. The modulation index (MI) was then calculated between

the phase of low-frequency rhythm and the high-frequency amplitude by computing the entropy values of this distribution and normalizing by the maximum entropy value (de Hemptinne et al., 2013, 2015; Tort et al., 2010). A mean modulation index was calculated for each data segment by averaging MI over the phase frequency range of 13–30 Hz (beta) and the amplitude frequency range of 50–200 Hz (broadband gamma).

Cortical PAC was calculated in a subset of subjects (n = 9) who experienced a long enough epoch of tremor to reliably calculate a phase-amplitude modulation index (~30 seconds, uninterrupted). Uninterrupted epochs were selected in order to minimize artifactual coupling stemming from edge effects. STN PAC and STN-M1 PAC were calculated in a different subset of patients (n = 8) who experienced long epochs of rest and tremor after lead insertion.

Statistical Analysis

The Kolmogorov-Smirnov test (MATLAB function kstest) rejected the null hypothesis that the paired differences being tested came from a normal distribution, so the nonparametric paired Wilcoxon signed-rank was used to evaluate differences between the rest and tremor conditions. All statistics were false discovery rate corrected for multiple comparisons, and the adjusted p values are presented here (Hochberg and Benjamini, 1990).

Surrogates were generated for coherence, PSI, AAC, and PAC analyses by shifting one signal by a randomly generated number of samples and using this shifted signal in analyses. These surrogate measures were calculated 300 times to establish a distribution for each patient. The 95th percentile of the distribution of these surrogate values was used as the threshold to determine significance.

RESULTS

Study subjects

Potential study subjects were characterized using the Unified Parkinson's Disease Rating Scale part III (UPDRS-III) following withdrawal of anti-parkinsonian medications for 12 hours. Subject inclusion criteria were as follows: age 21–75 years, normal brain magnetic resonance imaging (MRI) examination, sufficient disease severity in the setting of optimal medical management to justify treatment by DBS, and ability to cooperate during awake neurosurgery. Subjects were excluded if their recordings did not contain at least one epoch (defined as > 6 seconds) of spontaneous rest tremor, as well as a period of rest without tremor or other movement, during surgery. Thirty-three subjects met these criteria. Of these, 6 subjects had very low ECoG signal amplitudes (characterized by a root mean square amplitude <10 μV) or very low STN LFP signal amplitudes (characterized by a root mean square amplitude < 5 μV) and were therefore excluded from analysis. Mean age of studied subjects was 63 ± 8 years. Twenty-one subjects experienced at least one epoch of rest tremor and one of rest without tremor after ECoG placement and *prior* to lead insertion. Nine of these 21 subjects with pre-lead insertion rest tremor and rest without tremor experienced at least 30 second epochs of each condition, affording data segments of sufficient length to analyze cross frequency AAC and PAC in the cortex. *After* STN lead insertion, 10

experienced at least one epoch of rest tremor and of rest without tremor. Eight of these 10 subjects with post-lead insertion rest tremor and rest without tremor experienced at least 30 second epochs of each condition, affording data segments of sufficient length to analyze cross frequency AAC and PAC in the STN and between the STN and cortex. All antiparkinsonian medications were stopped 12 hours before the start of surgery. Median tremor frequency was 5.0 Hz ± 1.79 Hz. Characteristics of study subjects, and delineation of which study subjects contributed to each analysis, are provided in Table 1.

Tremor is associated with broad (8–55 Hz) desynchronization in M1

Tremor was associated with a significant decrease in alpha and beta power in both S1 (alpha: p<.05, beta: p<.01) and M1 (alpha: p<.05, beta: p<.001) compared to rest without tremor, and a significant decrease in low gamma power (30–55 Hz) exclusive to M1 (p<.05) (Figure 2A). In M1, alpha decreased in 16/21 subjects, beta decreased in 20/21 subjects (Figure 2C), and low gamma (30–55 Hz) decreased in 16/21 subjects. In S1, alpha decreased in 15/21 subjects, while beta decreased in 20/21 subjects, with no group difference in gamma. Neither theta (4–8 Hz) power nor broadband gamma (50–200 Hz) power changed during tremor (Figure 2A). Beta peak analysis revealed that maximum cortical beta amplitude decreased in M1 and S1 with tremor (p<0.05), though the width of the beta peak did not change significantly. We observed no peaks in other frequency ranges that appeared during tremor.

Low beta cortico-cortical coherence and phase synchronization decrease during tremor

Tremor was associated with a decrease in M1-S1 coherence that was restricted to the low beta range, from 13–20 Hz (p<0.05). This effect was observed in 15/21 subjects. There was no significant change in coherence in any other frequency band, including beta coherence taken as a whole (13–30 Hz) (Figure 3A). Peak coherence values, defined as the local maximums in a frequency range exceeding the surrogate threshold for significance, were examined as well. In 13/21 subjects there was peak in the beta frequency band during rest that disappeared during tremor. Additionally, in 13/21 subjects we observed a narrowband peak in the alpha frequency range that appeared during tremor, similar to the "double tremor frequency" activity that has been reported in MEG studies (Timmermann et al, 2003). This was not reflected in the averaged coherence data, which encompassed a wider frequency range than the narrowband peak.

To determine whether tremor-associated changes in coherence were driven primarily by phase effects or amplitude effects, we analyzed PSI and AAC in the frequency range that showed a tremor-associated reduction in coherence. Phase synchronization between M1 low beta and S1 low beta decreased during tremor (p<0.05). There was a strong correlation between the decrease in low beta M1-S1 coherence and this decrease in low beta M1-S1 PSI (R^2 = 0.64, p <.00001), indicating that the decrease in coherence was largely driven by a decrease in the phase synchronization. The preferred phase difference in the synchronized rest state varied from patient to patient (Figure 3D). The change in low beta M1-S1 coherence was also (more weakly) correlated with the change in low beta M1-S1 AAC (R^2 = 0.41, p <.01), but as there was no significant decrease in AAC during tremor it is unlikely that this was a driver of the tremor-associated changes in coherence.

Tremor decreases phase-amplitude coupling in M1

We previously showed that rigid-akinetic PD patients have exaggerated beta-gamma phase amplitude coupling (PAC) in M1, suggesting excessive synchronization of population spiking to the beta rhythm (de Hemptinne et al., 2013, 2015). Thus we sought to determine whether tremor had an effect on PAC. Out of 9 subjects with sufficiently long data segments to contribute to this analysis, 7 showed coupling of low frequency phase (alpha-beta) to high frequency amplitude (broadband gamma) (Figure 4A). Phase-amplitude coupling decreased significantly during tremor ($p < 0.05$) and this effect was observed in 7/9 subjects (Figure 4B). The other two subjects who showed no PAC at rest showed a slight increase in coupling during tremor, even though both subjects experienced a decrease in beta power. PAC was also examined in S1, but no significant coupling was found. Cross frequency AAC was also examined in these subjects, and yielded no significant change during tremor.

Tremor is associated with beta desynchronization in the STN

A subset of subjects (n=10) experienced sufficient epochs of rest and tremor after lead insertion allowing for simultaneous cortical and subcortical recordings. Analysis of STN LFP power revealed a decrease in beta power when subjects were experiencing tremor versus rest ($p<0.05$) (Figure 5A). This was seen in 8/10 subjects (Figure 5C). Comparisons at other frequency bands yielded no significant group differences, though we did note that 4/10 subjects showed a narrowband peak in spectral power ~ 9 Hz, approximately double the tremor frequency during, epochs of tremor. The maximum STN beta peak amplitude did not differ consistently between conditions, though peak width decreased significantly during tremor ($p<0.05$).

Alpha and beta coherence between M1 and STN decreases during tremor

During tremor, coherence between M1 and STN decreased in the alpha and beta frequency bands ($p<0.05$). This was the case in 9/10 subjects (Figure 5D). When examining the peak coherence values, we found that in most subjects there was a prominent broad peak in coherence in the alpha-beta range, and this peak did not change location during tremor but instead decreased in amplitude.

We did not find any significant changes in phase synchrony, amplitude-amplitude coupling, or phase amplitude coupling (Figure 4A) within STN or between cortex and STN. The decrease in alpha coherence between M1 and STN was not correlated with changes in alpha phase synchrony ($R^2 = 0.19$, $p > 0.05$), but was correlated with a decrease in alpha amplitude-amplitude coupling ($R^2 = 0.58$, $p <0.05$). The decrease in beta coherence between M1 and STN trended towards correlation with a decrease in phase synchrony ($R^2 = 0.44$, $p = 0.06$), and was not correlated with changes in amplitude-amplitude coupling. However, in the absence of a significant decrease in these measures, it is unclear whether phase or amplitude effects were the main drivers of the tremor-associated changes in M1-STN coherence.

DISCUSSION

In this study we examined the cortical and subcortical physiological correlates of parkinsonian rest tremor by analyzing intraoperative sensorimotor ECoG and STN LFP activity in subjects undergoing awake placement of DBS leads. We found that the spontaneous onset of tremor was associated with reduced alpha, beta, and low gamma power in M1, reduced M1 beta phase-gamma amplitude coupling, reduced beta power in the subthalamic nucleus, and reduced cortico-cortical and cortico-subthalamic beta coherence. High gamma (broadband) power in sensorimotor cortex, normally increased during voluntary movement (Crone et al., 1998a; Miller et al., 2009), did not change during tremor.

Tremor reduces pathological synchronization in the beta band

It has long been known that movement is associated with an alpha-beta event related desynchronization (ERD) in the cortex and subthalamic nucleus. This has been shown for self-paced voluntary movement (Crone et al., 1998b) passive movement (Alegre et al. 2006; Formaggio et al., 2013), and imagined movement (Formaggio et al., 2013). Alpha-beta ERD is typically represented broadly across the sensorimotor cortex (Pfurtscheller et al., 2003), occurs prior to movement initiation, and is thought to represent a "pro-kinetic" state of increased cortical responsiveness (Crone et al., 1998b). One theory of the pathophysiology of parkinsonian akinesia and bradykinesia is that these motor signs are generated by increased oscillatory synchronization in the basal-ganglia thalamocortical loop in the beta band. Manifestations of this may include increased cortico-cortical coherence (Silberstein et al., 2005), increased cortico-subthalamic coherence (Fogelson et al., 2006) and increased synchronization of neuronal spiking to a specific phase of the beta rhythm (Kuhn et al., 2005, Moran et al., 2008; de Hemptinne et al., 2013). Cortical beta-gamma phase amplitude coupling is one metric of synchronization of neuronal populations to the beta rhythm, since cortical high gamma activity is a surrogate marker for population spiking (Manning et al., 2009).

Here, we show that tremor onset reduces many of these metrics of elevated beta band synchrony, suggesting that tremor may actually partly suppress the physiological drivers of bradykinesia/akinesia. This may account for the clinical observation that parkinsonian tremor over time is often "dissociated" from that of bradykinesia/akinesia; as the latter positively correlates with degree of dopaminergic neuronal loss while the former does not. It is possible that only some patients are able to engage the compensatory circuit responsible for tremor generation, which may include the motor cortex and cerebellum, and that disease progression gradually disrupts the circuit's ability to compensate (Helmich et al., 2012). This could explain why tremor can decrease in severity with increased DA loss (Toth et al., 2004) or disappear entirely (Hughes et al. 1993).

The current study is limited to patients who experience tremor as one of their cardinal PD motor signs, necessarily excluding comparisons with patients with a pure rigid/bradykinetic phenotype who do not experience tremor. Comparing metrics of beta synchrony in patients with rigid-akinetic PD against those in tremor-dominant PD would be useful to further test the hypothesis that tremor is partly compensatory for elevated beta band synchronization.

Another implication of these findings is that metrics of excessive beta oscillatory synchronization might not serve as optimal control signals for closed-loop DBS in PD patients, as has been previously proposed (Little et al., 2013), if the patient has prominent tremor. In these patients, an additional biomarker for tremor must be taken into account.

Motor cortex activation in broadband gamma distinguishes voluntary movement from tremor

Although tremor and normal voluntary movement show physiological overlap with respect to their associated changes in cortical beta band synchronization, this does not seem to be the case for higher frequency, broadband phenomena. Broadband gamma (50–200 Hz) is a non-oscillatory physiological signal that we take as a surrogate measure for local population spiking and afferent activity (Manning et al., 2009; Suffczynski et al., 2014). Voluntary movement has been shown to increase power in the broadband gamma frequency range (Crone et al., 1998a; Miller et al., 2007, 2008, 2009; Manning et al., 2009) in ECoG recordings over sensorimotor cortex. Therefore, the voluntary movement-related broadband gamma response may indicate a functional increase in M1 neuronal recruitment. If M1 played the same role in generating both tremor and non-tremor movement, then we would expect to see an increase in broadband gamma power during tremor. However, we found no increase in broadband gamma power in M1, S1, or STN during tremor, even though broadband increases have been shown in other patients with PD during simple voluntary arm movements (Crowell et al., 2012). Our results indicate a physiological distinction between tremor and non-tremor movement identifiable in motor cortex, and support the idea that M1 activation is not necessary for tremor genesis.

Comparison to prior physiological studies of parkinsonian tremor

Several prior publications have explored the cortical physiological correlates of parkinsonian tremor using MEG (Timmermann et al., 2003; Volkmann et al., 1996), EEG (Hellwig et al., 2000), STN LFP (Wang et al., 2005), or MEG combined with STN LFP recording (Hirschmann et al., 2013). Several of these have shown tremor to be associated with the emergence of a "double tremor frequency" (9–11 Hz) peak in cortico-cortical coherence. Our findings, utilizing a distinct technical approach based on ECoG, are largely consistent with prior studies, in many but not all of our subjects. We also found that a small narrowband peak in cortico-cortical alpha coherence, or the "double tremor frequency" range appeared in 13/21 subjects during tremor (Timmermann et al., 2003). Additionally, a recent MEG study by Hirschmann et al. (2013) found a cortical beta ERD during PD rest tremor, consistent with the present study. One prior study found increased theta power in the STN during tremor, which we did not find (Hirschmann et al., 2013). This is likely because increased theta was found exclusively 5–9 seconds after the onset of tremor, and we did not control for the timing of the effects we observed with relation to tremor onset.

Another study found increased low gamma power (35–55 Hz) in the STN during tremor (Weinberger et al., 2009). Of note, this increase was in a relatively narrow frequency band, likely arising from a low gamma oscillatory rhythm, which is physiologically distinct from the *broadband* gamma discussed above. Recent work has also shown that STN DBS-induced suppression of tremor was associated with a reduction in the same low gamma oscillations

Author Manuscript

Author Manuscript

Author Manuscript

Author Manuscript

(Beudel et al., 2015). Although here we did not find a tremor-associated increase in a low gamma rhythm in STN, this may reflect the relatively small number of subjects who provided STN data (compared with cortical data obtained prior to insertion of the STN lead), or the "microlesion" effect associated with acute STN lead insertion.

Limitations

All data reported in this study came from intraoperative recording, and relied on the spontaneous appearance and disappearance of rest tremor, limiting the amount of time in which recordings could take place. To include a sufficient number of subjects, we had to select a relatively short epoch length for our analyses. Because quantification of cross frequency analyses such as phase-amplitude coupling and cross frequency amplitude-amplitude coupling requires a somewhat longer data segment, we only analyzed cross frequency interactions in a subset of subjects with sufficiently long recordings for this analysis. Also, because we did not systematically record during voluntary movement in this patient cohort, we were unable to directly compare the network changes associated with tremor onset to those related to voluntary movement. Another limitation is that, for analyses of cortico-subthalamic coherence or STN oscillatory activity, data were necessarily collected after insertion of the DBS lead in the STN, which can result in symptom improvement through a "microlesion" effect (Koop et al., 2006). This may explain why only 10 subjects experienced tremor after lead insertion. Additionally, differences in recording systems as well as electrode size and spacing increased data set variability, though we did not observe any specific trends with respect to electrode type or recording system.

Conclusions

Tremor reduces beta band synchronization within and between structures of the basal ganglia thalamocortical motor network. Our findings support the hypothesis that rest tremor in PD may partly compensates for the excessive beta synchronization in this loop that is thought to drive akinesia and bradykinesia. These compensatory network dynamics may underlie observed differences in the evolution of tremor, compared to other motor signs, in the progression of Parkinson's disease.

ACKNOWLEDGMENTS

REFERENCES

Alegre M, Labarga A, Gurtubay IG, Iriarte J, Malanda A, Artieda J. Beta electroencephalograph changes during passive movements: sensory afferences contribute to beta event-related desynchronization in humans. Neurosci Lett. 2002; 331:29–32. [PubMed: 12359316]

Beudel M, Little S, Pogosyan A, Ashkan K, Foltynie T, Limousin P, Zrinzo L, Hariz M, Bogdanovic M, Cheeran B, Green A, Aziz T, Thevathasan W, Brown P. Tremor reduction by deep brain stimulation is associate with gamma power suppression in Parkinson's disease. Neuromodulation: Technology at the Neural Interface. 2015; 18(5):349–354.

Bruns A, Eckhorn R, Jokeit H, Ebner A. Amplitude envelope correlation detects coupling among incoherent brain signals. Neuroreport. 2000; 11:1509–1514. [PubMed: 10841367]

Cagnan H, Little S, Foltynie T, Limousin P, Zrinzo L, Hariz M, Cheeran B, Fitzgerald J, Green AL, Aziz T, Brown P. The nature of tremor circuits in parkinsonian and essential tremor. Brain. 2014; 137:3223–3234. [PubMed: 25200741]

Crone NE, Miglioretti DL, Gordon B, Lesser RP. Functional mapping of human sensorimotor cortex with electrocorticographic spectral analysis. II. Event-related synchronization in the gamma band. Brain. 1998a; 121(Pt 12):2301–2315. [PubMed: 9874481]

Crone NE, Miglioretti DL, Gordon B, Sieracki JM, Wilson MT, Uematsu S, Lesser RP. Functional mapping of human sensorimotor cortex with electrocorticographic spectral analysis. I. Alpha and beta event-related desynchronization. Brain. 1998b; 121(Pt 12):2271–2299. [PubMed: 9874480]

Crowell AL, Ryapolova-Webb ES, Ostrem JL, Galifianakis NB, Shimamoto S, Lim DA, Starr PA. Oscillations in sensorimotor cortex in movement disorders: an electrocorticography study. Brain. 2012; 135:615–630. [PubMed: 22252995]

de Hemptinne C, Ryapolova-Webb ES, Air EL, Garcia PA, Miller KJ, Ojemann JG, Ostrem JL, Galifianakis NB, Starr PA. Exaggerated phase-amplitude coupling in the primary motor cortex in Parkinson disease. Proc Natl Acad Sci U S A. 2013; 110:4780–4785. [PubMed: 23471992]

de Hemptinne C, Swann NC, Ostrem JL, Ryapolova-Webb ES, San Luciano M, Galifianakis NB, Starr PA. Therapeutic deep brain stimulation reduces cortical phase-amplitude coupling in Parkinson's disease. Nat Neurosci. 2015; 18:779–786. [PubMed: 25867121]

Delorme A, Makeig S. EEGLAB: an open source toolbox for analysis of single-trial EEG dynamics including independent component analysis. J Neurosci Methods. 2004; 134:9–21. [PubMed: 15102499]

Fogelson N, Williams D, Tijssen M, van Bruggen G, Speelman H, Brown P. Different functional loops between cerebral cortex and the subthalmic area in Parkinson's disease. Cereb Cortex. 2006; 16:64–75. [PubMed: 15829734]

Formaggio E, Storti SF, Boscolo Galazzo I, Gandolfi M, Geroin C, Smania N, Spezia L, Waldner A, Fiaschi A, Manganotti P. Modulation of event-related desynchronization in robot-assisted hand performance: brain oscillatory changes in active, passive and imagined movements. J Neuroeng Rehabil. 2013; 10:24. [PubMed: 23442349]

Hammond C, Bergman H, Brown P. Pathological synchronization in Parkinson's disease: networks, models and treatments. Trends Neurosci. 2007; 30:357–364. [PubMed: 17532060]

Hellwig B, Haussler S, Lauk M, Guschlbauer B, Koster B, Kristeva-Feige R, Timmer J, Lucking CH. Tremor-correlated cortical activity detected by electroencephalography. Clin Neurophysiol. 2000; 111:806–809. [PubMed: 10802450]

Helmich RC, Hallett M, Deuschl G, Toni I, Bloem BR. Cerebral causes and consequences of parkinsonian resting tremor: a tale of two circuits? Brain. 2012; 135:3206–3226. [PubMed: 22382359]

Hirschmann J, Hartmann CJ, Butz M, Hoogenboom N, Ozkurt TE, Elben S, Vesper J, Wojtecki L, Schnitzler A. A direct relationship between oscillatory subthalamic nucleus-cortex coupling and rest tremor in Parkinson's disease. Brain. 2013; 136:3659–3670. [PubMed: 24154618]

Hochberg Y, Benjamini Y. More powerful procedures for multiple significance testing. Stat Med. 1990; 9:811–818. [PubMed: 2218183]

Hoehn MM, Yahr MD. Parkinsonism: onset, progression and mortality. Neurology. 1967; 17:427–442. [PubMed: 6067254]

Hughes AJ, Daniel SE, Blankson S, Lees AJ. A clinicopathologic study of 100 cases of Parkinson's disease. Arch Neurol. 1993; 50:140–148. [PubMed: 8431132]

Hutchison WD, Lozano AM, Tasker RR, Lang AE, Dostrovsky JO. Identification and characterization of neurons with tremor-frequency activity in human globus pallidus. Exp Brain Res. 1997; 113:557–563. [PubMed: 9108220]

Koop MM, Andrzejewski A, Hill BC, Heit G, Bronte-Stewart HM. Improvement in a quantitative measure of bradykinesia after microelectrode recording in patients with Parkinson's disease during deep brain stimulation surgery. Mov Disord. 2006; 21:673–678. [PubMed: 16440333]

Kuhn AA, Trottenberg T, Kivi A, Kupsch A, Schneider G, Brown P. The relationship between local field potential and neuronal discharge in the subthalamic nucleus of patients with Parkinson's disease. Exp Neurol. 2005; 194:212–220. [PubMed: 15899258]

Levy R, Ashby P, Hutchison WD, Lang AE, Lozano AM, Dostrovsky JO. Dependence of subthalamic nucleus oscillations on movement and dopamine in Parkinson's disease. Brain. 2002; 125:1196–1209. [PubMed: 12023310]

Levy R, Hutchison WD, Lozano AM, Dostrovsky JO. High-frequency synchronization of neuronal activity in the subthalamic nucleus of parkinsonian patients with limb tremor. J Neurosci. 2000; 20:7766–7775. [PubMed: 11027240]

Little S, Tan H, Anzak A, Pogosyan A, Kuhn A, Brown P. Bilateral functional connectivity of the basal ganglia in patients with Parkinson's disease and its modulation by dopaminergic treatment. PLoS One. 2013; 8:e82762. [PubMed: 24376574]

Louis ED, Tang MX, Cote L, Alfaro B, Mejia H, Marder K. Progression of parkinsonian signs in Parkinson disease. Arch Neurol. 1999; 56:334–337. [PubMed: 10190824]

Mann JM, Foote KD, Garvan CW, Fernandez HH, Jacobson CEt, Rodriguez RL, Haq IU, Siddiqui MS, Malaty IA, Morishita T, Hass CJ, Okun MS. Brain penetration effects of microelectrodes and DBS leads in STN or GPi. J Neurol Neurosurg Psychiatry. 2009; 80:794–797. [PubMed: 19237386]

Manning JR, Jacobs J, Fried I, Kahana MJ. Broadband shifts in local field potential power spectra are correlated with single-neuron spiking in humans. J Neurosci. 2009; 29:13613–13620. [PubMed: 19864573]

Miller KJ, Leuthardt EC, Schalk G, Rao RP, Anderson NR, Moran DW, Miller JW, Ojemann JG. Spectral changes in cortical surface potentials during motor movement. J Neurosci. 2007; 27:2423–2432.

Miller KJ, Shenoy P, den Nijs M, Sorensen LB, Rao RP, Ojemann JG. Beyond the gamma band: the role of high-frequency features in movement classification. IEEE Trans Biomed Eng. 2008; 55:1634–1637. [PubMed: 18440909]

Miller KJ, Zanos S, Fetz EE, den Nijs M, Ojemann JG. Decoupling the cortical power spectrum reveals real-time representation of individual finger movements in humans. J Neurosci. 2009; 29:3132–3137. [PubMed: 19279250]

Moran RJ, Stephan KE, Kiebel SJ, Rombach N, O'Connor WT, Murphy KJ, Reilly RB, Friston KJ. Bayesian estimation of synaptic physiology from the spectral responses of neural masses. Neuroimage. 2008; 42:272–284. [PubMed: 18515149]

Panov F, Levin E, de Hemptinne C, Swann NC, Qasim SE, Miocinovic S, Ostrem JL, Starr PA. Intraoperative electrocorticography for physiological research in movement disorders: principles and experience in 200 cases. J Neurosurg. 2015 *In press*.

Pfurtscheller G, Graimann B, Huggins JE, Levine SP, Schuh LA. Spatiotemporal patterns of beta desynchronization and gamma synchronization in corticographic data during self-paced movement. Clin Neurophysiol. 2003; 114:1226–1236. [PubMed: 12842719]

Pirker W. Correlation of dopamine transporter imaging with parkinsonian motor handicap: how close is it? Mov Disord. 2003; 18(Suppl 7):S43–S51. [PubMed: 14531046]

Reck C, Florin E, Wojtecki L, Krause H, Groiss S, Voges J, Maarouf M, Sturm V, Schnitzler A, Timmermann L. Characterisation of tremor-associated local field potentials in the subthalamic nucleus in Parkinson's disease. Eur J Neurosci. 2009; 29:599–612. [PubMed: 19187268]

Shahlaie K, Larson PS, Starr PA. Intraoperative computed tomography for deep brain stimulation surgery: technique and accuracy assessment. Neurosurgery. 2011; 68:114–124. discussion 124. [PubMed: 21206322]

Shimamoto SA, Ryapolova-Webb ES, Ostrem JL, Galifianakis NB, Miller KJ, Starr PA. Subthalamic nucleus neurons are synchronized to primary motor cortex local field potentials in Parkinson's disease. J Neurosci. 2013; 33:7220–7233. [PubMed: 23616531]

Silberstein P, Pogosyan A, Kuhn AA, Hotton G, Tisch S, Kupsch A, Dowsey-Limousin P, Hariz MI, Brown P. Cortico-cortical coupling in Parkinson's disease and its modulation by therapy. Brain. 2005; 128:1277–1291. [PubMed: 15774503]

Starr PA, Christine CW, Theodosopoulos PV, Lindsey N, Byrd D, Mosley A, Marks WJ Jr. Implantation of deep brain stimulators into the subthalamic nucleus: technical approach and magnetic resonance imaging-verified lead locations. J Neurosurg. 2002; 97:370–387. [PubMed: 12186466]

Timmermann L, Gross J, Dirks M, Volkmann J, Freund HJ, Schnitzler A. The cerebral oscillatory network of parkinsonian resting tremor. Brain. 2003; 126:199–212. [PubMed: 12477707]

Tort AB, Komorowski R, Eichenbaum H, Kopell N. Measuring phase-amplitude coupling between neuronal oscillations of different frequencies. J Neurophysiol. 2010; 104:1195–1210. [PubMed: 20463205]

Toth C, Rajput M, Rajput AH. Anomalies of asymmetry of clinical signs in parkinsonism. Mov Disord. 2004; 19:151–157. [PubMed: 14978669]

Tykocki T, Nauman P, Koziara H, Mandat T. Microlesion effect as a predictor of the effectiveness of subthalamic deep brain stimulation for Parkinson's disease. Stereotact Funct Neurosurg. 2013; 91:12–17. [PubMed: 23154788]

Volkmann J, Joliot M, Mogilner A, Ioannides AA, Lado F, Fazzini E, Ribary U, Llinas R. Central motor loop oscillations in parkinsonian resting tremor revealed by magnetoencephalography. Neurology. 1996; 46:1359–1370. [PubMed: 8628483]

Wang S, Aziz TZ, Stein JF, Liu X. Time-frequency analysis of transient neuromuscular events: dynamic changes in activity of the subthalamic nucleus and forearm muscles related to the intermittent resting tremor. J Neurosci Meth. 2005; 145:151–158.

Weinberger M, Hutchison WD, Lozano AM, Hodaie M, Dostrovsky JO. Increased gamma oscillatory activity in the subthalamic nucleus during tremor in Parkinson's disease patients. J Neurophysiol. 2009; 101:789–802. [PubMed: 19004998]

Yanagisawa T, Yamashita O, Hirata M, Kishima H, Saitoh Y, Goto T, Yoshimine T, Kamitani Y. Regulation of motor representation by phase-amplitude coupling in the sensorimotor cortex. J Neurosci. 2012; 32:15467–15475. [PubMed: 23115184]

Yousry TA, Schmid UD, Alkadhi H, Schmidt D, Peraud A, Buettner A, Winkler P. Localization of the motor hand area to a knob on the precentral gyrus. A new landmark. Brain. 1997; 120(Pt 1):141–157. [PubMed: 9055804]

Zaidel A, David A, Zvi I, Bergman H. Akineto-rigid vs. tremor syndromes in parkinsonism. Current Opinion in Neurology. 2009; 22(4):387–393. [PubMed: 19494773]

Highlights

- We recorded cortical ECoG and STN LFP in PD patients during rest tremor.

- Rest tremor decreased beta synchronization in the basal ganglia-cortical loop.

- Cortical activity during rest tremor may distinguish tremor from voluntary movement.

- Rest tremor may partly compensate for excessive beta band synchronization in PD.
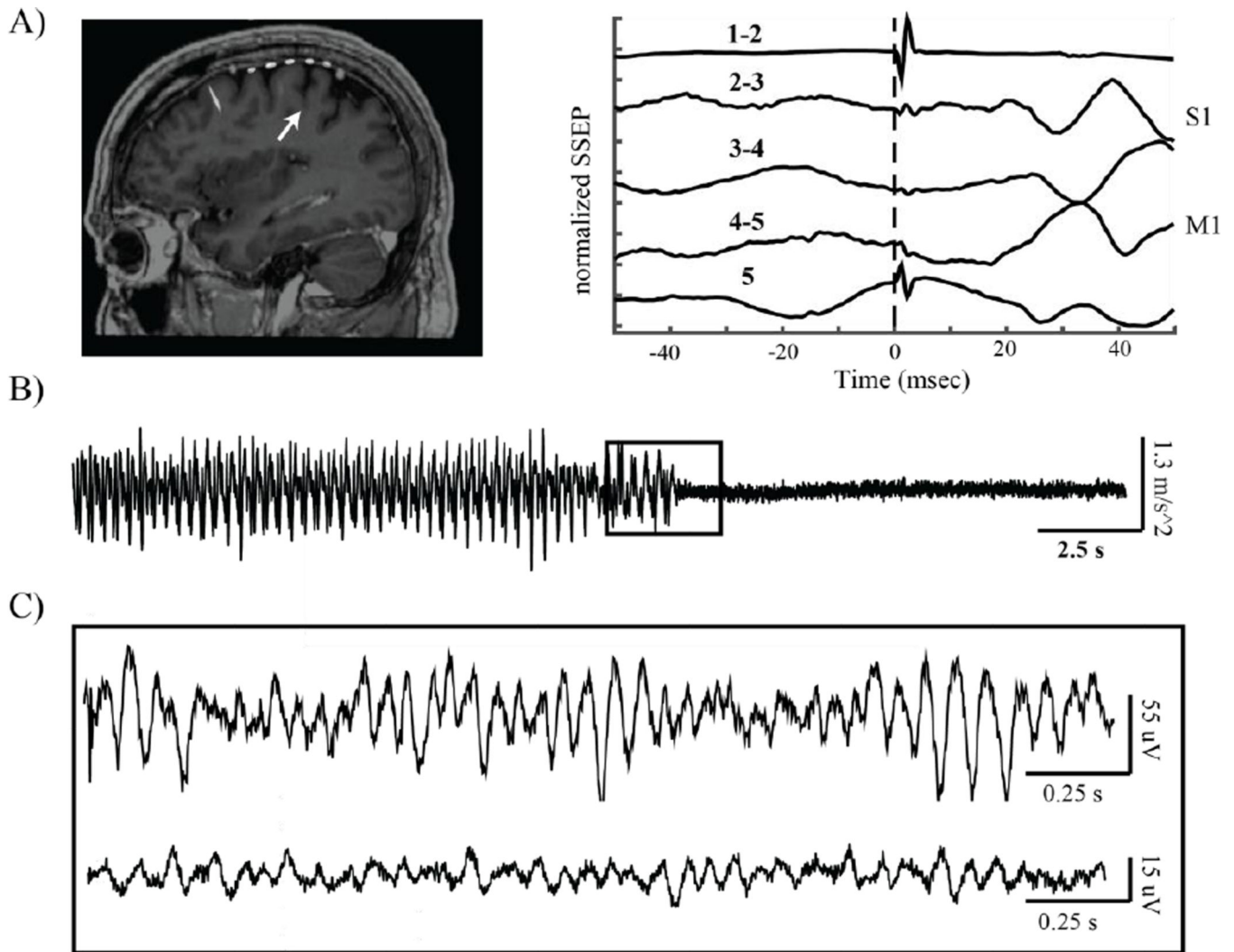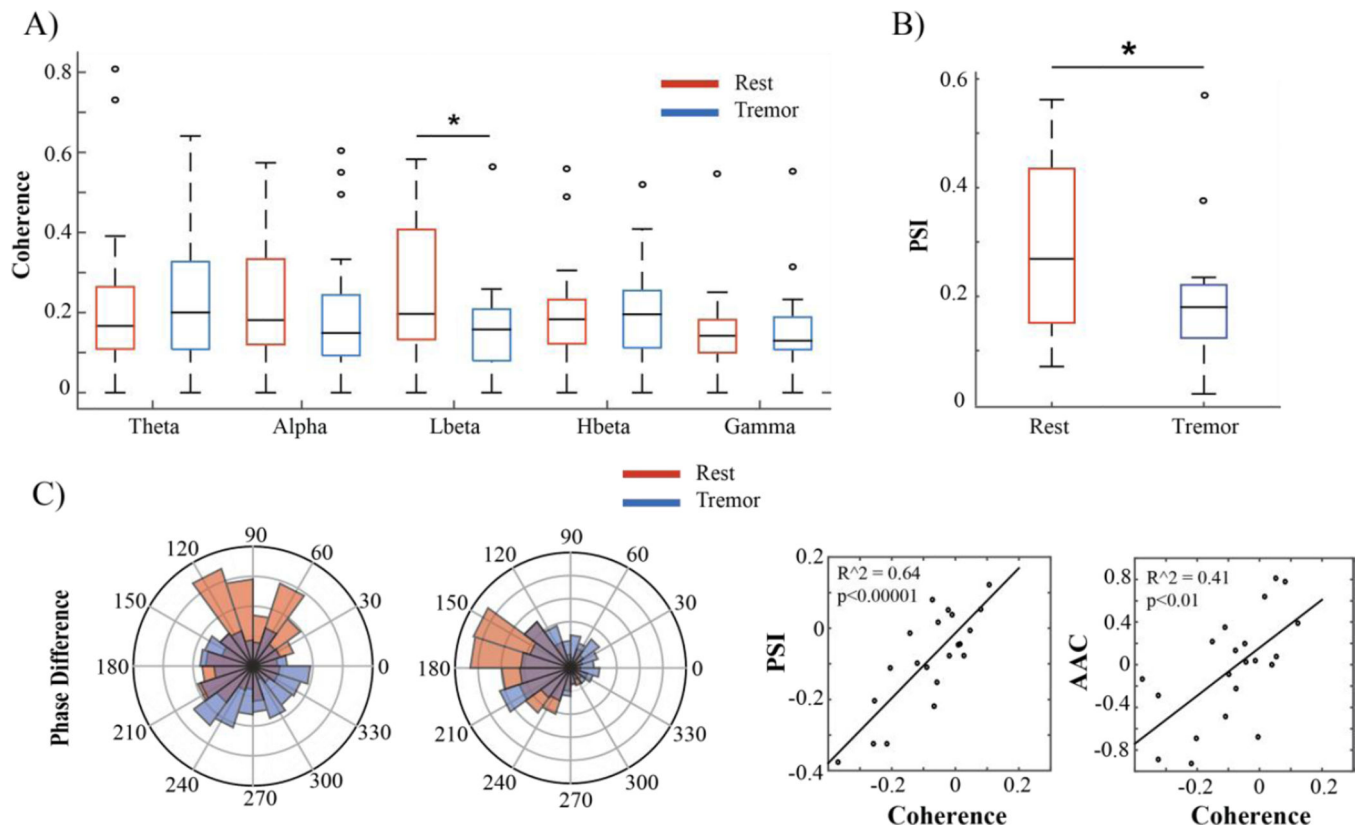
Figure 1.
Data recording methods. A) From left to right: intraoperative MRI/CT fusion showing placement of subdural 6 contact strip over sensorimotor cortex, with arrow pointing to the central sulcus. Median nerve somatosensory evoked potential (SSEP) showing reversal of the N20 potential at the electrode contact pair spanning the primary motor cortex (M1). B) Example accelerometer data obtained from one patient experiencing an epoch of rest tremor, which ended suddenly. C) Example brain recordings corresponding to accelerometer data presented indicated by inset in (B). Top: ECoG data obtained from the contacts spanning M1. Bottom: Simultaneously recorded LFP from two contacts in the dorsal subthalamic nucleus.
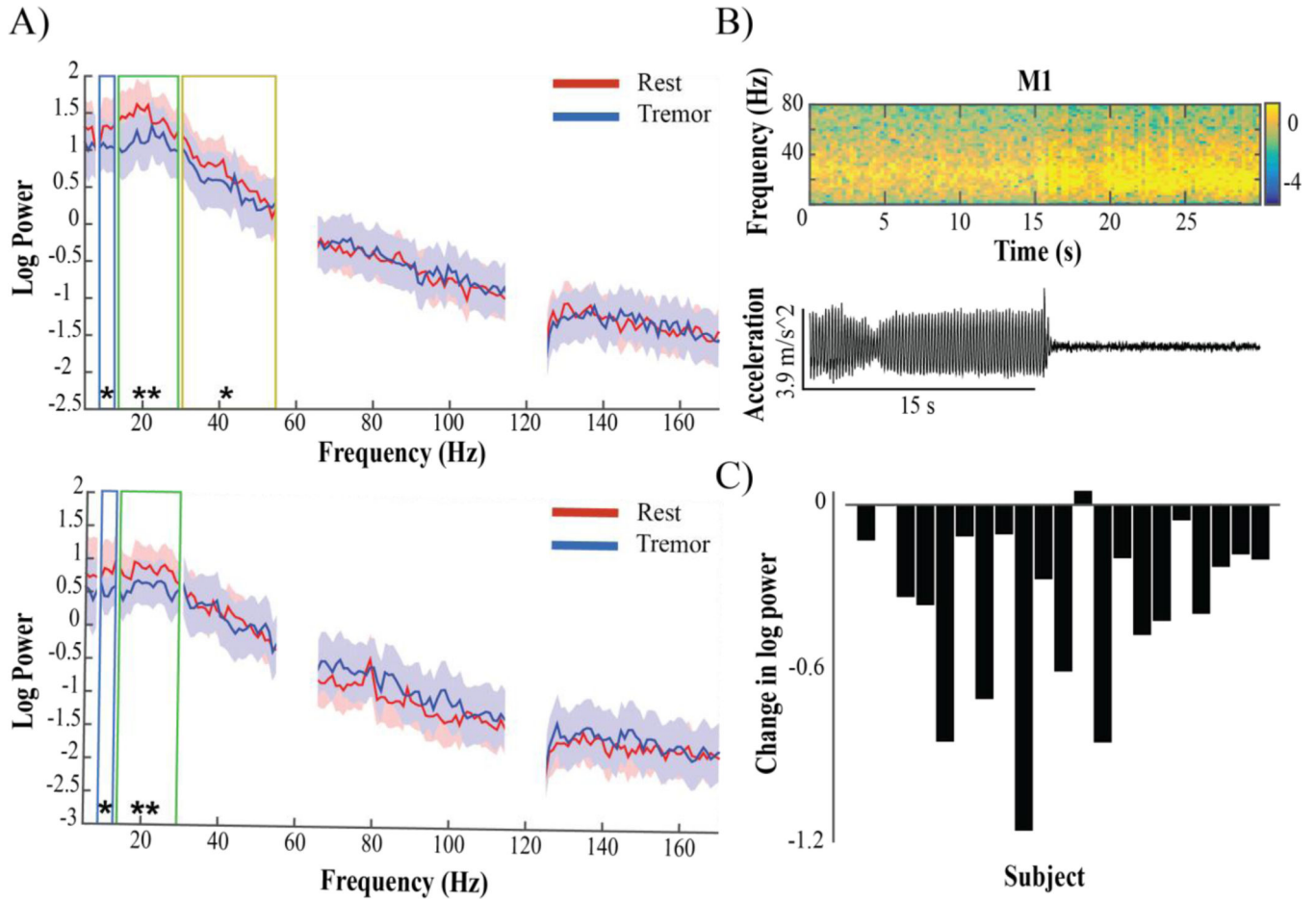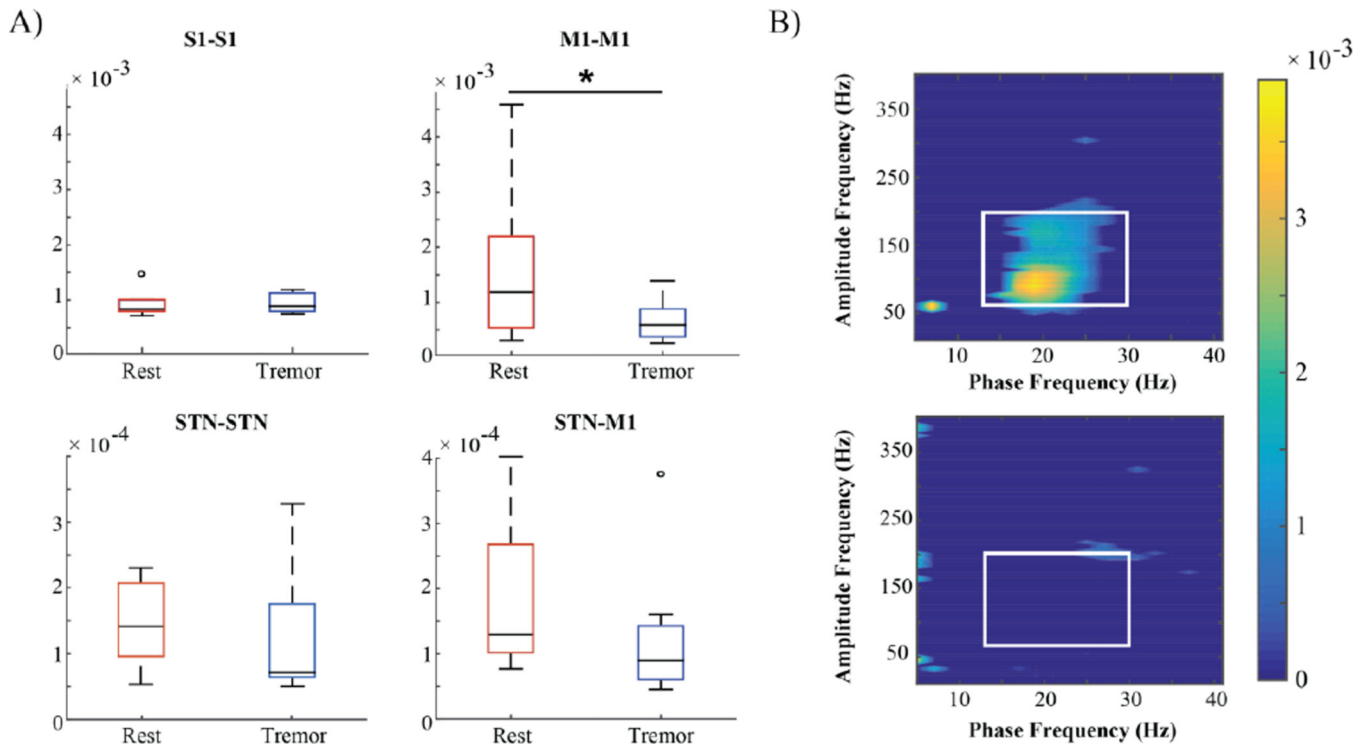
Figure 2.
Spectral changes in M1 and S1 associated with rest tremor. A) M1 (top) and S1 (bottom) median log power spectral density of patients (n=23) during rest without movement (red) and rest tremor (blue). Shading indicates interquartile range (IQR). Boxes correspond to frequency bands in which a significant change was seen: blue – alpha, green – beta, yellow – low gamma. There was no significant difference at any frequency range above low gamma for M1, or above beta for S1. B) Top: Example spectrogram showing timing of log power changes in M1 in one patient relative to tremor offset, seen below in corresponding accelerometer trace. Warmer colors indicate higher values, cooler colors indicate lower values. Most instances of tremor had a more gradual onset and/or offset. C) M1 log beta power difference between conditions in each subject (Tremor-Rest).
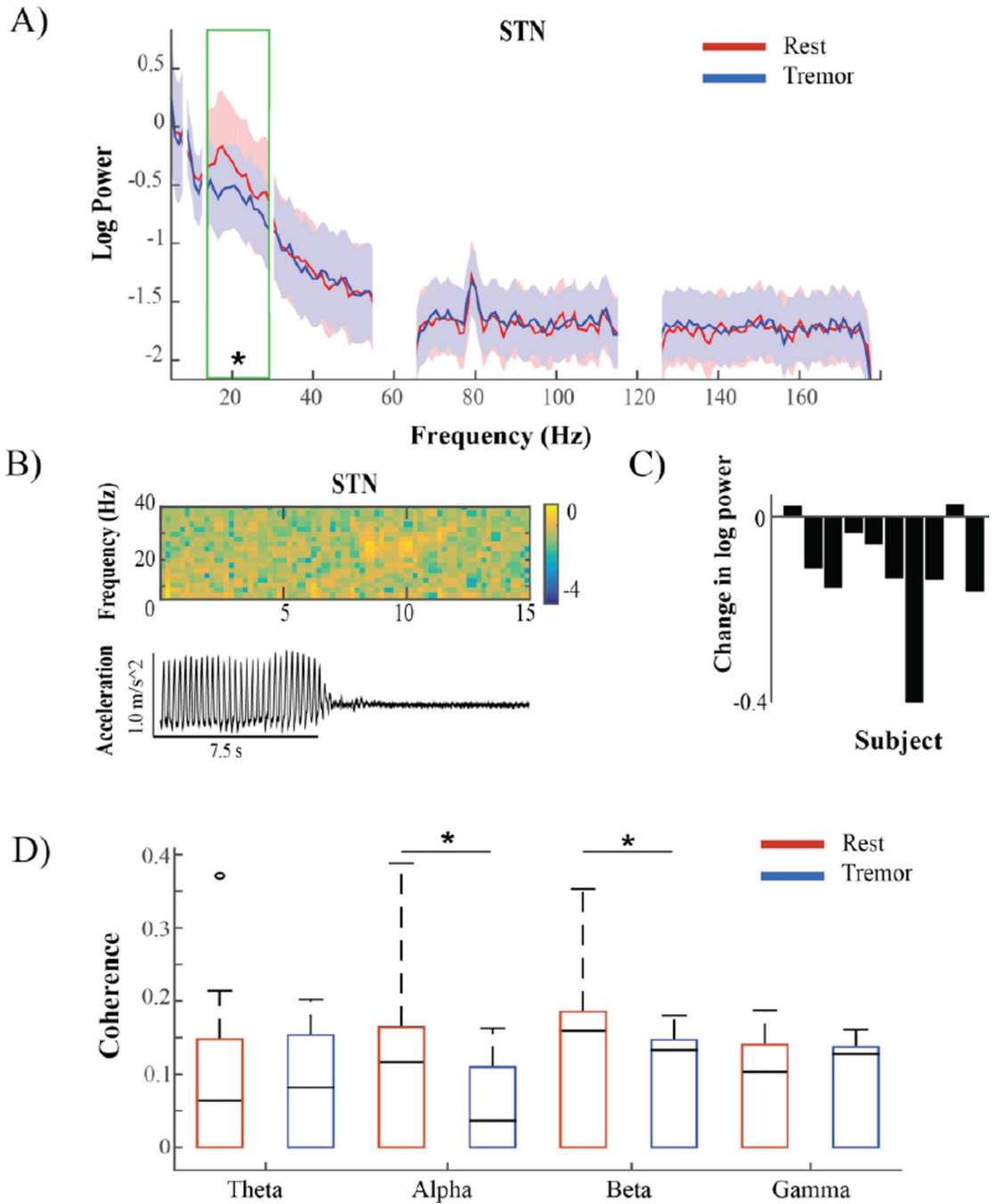
Figure 3.
Cortico-cortical coherence and phase synchrony changes associated with rest tremor. A) Box and whisker plots of magnitude squared coherence between M1 and S1 in different frequency ranges. The boxes represent the second and third quartiles, separated by a black line representing the median. The length of the whiskers is equal to 1.5× the interquartile range (IQR). Open circles represent values beyond 1.5× the IQR. Subjects exhibited a significant decrease in low beta coherence during tremor (blue) when compared to rest (red). B) Low beta PSI between M1 and S1. No other significant differences in cortico-cortical phase synchronization were found. C) Left: Two examples of preferred phase difference between M1 and S1 during rest (red) and tremor (blue). The preferred phase difference at rest was not constant between subjects. Right: Correlation between change in cortico-cortical coherence and cortico-cortical PSI and AAC in the low beta band. Each dot represents the values for one subject.

Figure 4.
Cortical phase-amplitude coupling (PAC) decreases during rest tremor. A) S1-S1 (n = 9), M1-M1 (n = 9), STN-STN (n = 8), STN-M1 (n = 8) phase-amplitude coupling averaged across beta phase and broadband gamma amplitude. There was a significant decrease only in M1-M1 PAC. B) Top: M1-M1 phase-amplitude coupling in one patient during rest. Warm colors indicate higher values for the modulation index (MI), cool colors indicate lower values. For grouped comparisons, MI was averaged across the values framed by the white box (13–30 Hz for phase, 70–200 Hz for amplitude). Bottom: M1-M1 phase-amplitude coupling in the same patient during tremor.

Figure 5.

Tremor associated changes in STN power and connectivity. A) STN median log power spectral density of patients (n=10) during rest without movement (red) and rest tremor (blue). Shading indicates interquartile range (IQR). The green box corresponds to the beta frequency band in which a significant change was seen. B) Top: Example spectrogram showing timing of log power changes in STN in one patient relative to tremor offset, seen below in corresponding accelerometer trace. Warmer colors indicate higher values, cooler colors indicate lower values. C) Log beta power difference between conditions in each

subject (Tremor-Rest). D) Magnitude squared coherence between M1 and STN in different frequency ranges. Subjects exhibited a significant decrease in alpha and beta coherence during tremor (blue) when compared to rest (red).

Author Manuscript   Author Manuscript   Author Manuscript   Author Manuscript

Table 1

Patient demographics

Subject	Age	Data Contribution	Gender	Brain Side Recorded	UPDRS III (OFF)	UPDRS III (ON)
1	68	Pre *	M	L	47	29
2	64	Pre *	M	R	37	21
3	54	Pre	M	R	55	29
4	70	Pre	M	R	17	2
5	50	Pre, Post **	F	L	37	10
6	63	Pre *	M	R	47	39
7	75	Pre	M	R	33	N/A
8	60	Pre	M	L	47	16
9	58	Pre *	M	R	37	24
10	61	Pre	M	R	35	5
11	66	Pre *	M	R	60	27
12	61	Pre *	M	R	40	31
13	63	Pre *	M	R	48	32
14	61	Pre *	F	L	40	21
15	72	Pre	M	R	50	N/A
16	68	Pre, Post **	M	L	49	35
17	78	Pre	M	R	39	28
18	68	Pre, Post **	M	L	58	42
19	70	Pre, Post **	M	R	N/A	N/A
20	55	Pre	M	L	43	10
21	61	Pre *	M	L	22	11
22	48	Post **	M	R	32	9
23	54	Post **	M	L	37	14
24	62	Post	F	R	32	6

Subject	Age	Data Contribution	Gender	Brain Side Recorded	UPDRS III (OFF)	UPDRS III (ON)
25	79	Post **	M	L	46	20
26	54	Post	M	L	42	23
27	56	Post **	M	R	21	10

Pre and Post denote patients who contributed to prelead (n = 21) and/or postlead (n=10) power, coherence, PSI, and within-frequency AAC analyses.

*
These patients (n = 9) had data segments of sufficient length to contribute to M1-M1, S1-S1, and M1-S1 PAC and cross frequency AAC analyses.

**
These patients (n = 8) had data segments of sufficient length to contribute to STN-STN and STN-M1 PAC and cross frequency AAC analyses.